

# Modulating F-actin organization induces organ growth by affecting the Hippo pathway

Leticia Sansores-Garcia, Wouter Bossuyt, Ken-Ichi Wada, Shigenobu Yonemura, Chunyao Tao, Hiroshi Sasaki and Georg Halder

This file contains Supplemental information and Supplemental figure legends.

## **Supplemental Information: Detailed genotypes used in the figures.**

### Figure 2:

(A) *w;;hh-Gal4, UAS-GFP/+*, (B) *w;;dpp-Gal4, UAS-GFP/+*, (C) *w;30A-Gal4/UAS-GFP*; (D) *yw*, (E-F) *yw; UAS-cpa<sup>RNAi</sup>/+; hh-Gal4, UAS-GFP/+*, (G-H) *yw;; dpp-Gal4, UAS-GFP/UAS-dia<sup>CA</sup>*, (I-J) *yw; 30A-Gal4/+; UAS-dia<sup>CA</sup>/UAS-GFP*.

### Figure 3:

(A) *yw; ex<sup>697</sup>/+; hh-Gal4, UAS-GFP/+*, (B) *yw; UAS-cpa<sup>RNAi</sup>/ex<sup>697</sup>; hh-Gal4, UAS-GFP/+*, (C) *yw; 30A-Gal4/ex<sup>697</sup>; UAS-dia<sup>CA</sup>/UAS-GFP*, (D) *yw; ex<sup>697</sup>/+; dpp-Gal4, UAS-GFP/UAS-dia<sup>CA</sup>*, (E) *yw*, (F) *yw; UAS-cpa<sup>RNAi</sup>/+; hh-Gal4, UAS-GFP/+*, (G) *yw;; dpp-Gal4, UAS-GFP/UAS-dia<sup>CA</sup>*, (H) *yw; 30A-Gal4/+; UAS-dia<sup>CA</sup>/+*. (I) *yw, hs-flp; act<CD2<Gal4, UAS-GFP/UAS-cpa<sup>RNAi</sup>, UAS-bsk<sup>DN</sup>/+*

### Figure 4:

(A) *w; gmr-Gal4/+*; (B) *w; gmr-Gal4/+; UAS-dia<sup>CA</sup>/+*, (C) *w; gmr-Gal4/yki<sup>B5</sup>; UAS-dia<sup>CA</sup>/+*, (E) *yw; UAS-cpa<sup>RNAi</sup>/+; hh-Gal4, UAS-GFP/+*, (F) *yw; ex<sup>697</sup>/+; hh-Gal4, UAS-GFP/UAS-yki<sup>RNAi</sup>*, (G) *yw; UAS-cpa<sup>RNAi</sup>/ex<sup>697</sup>; hh-Gal4, UAS-GFP/UAS-yki<sup>RNAi</sup>*, (H) *yw; ex<sup>697</sup>/+; dpp-Gal4, UAS-GFP/ UAS-yki<sup>RNAi</sup>*, (I) *yw; ex<sup>697</sup>/+; dpp-Gal4, UAS-GFP/UAS, dia<sup>CA</sup>, UAS-yki<sup>RNAi</sup>*.

Figure 5:

(A) *yw; UAS-ex/ex<sup>697</sup>; dpp-Gal4, UAS-GFP/+*, (B) *yw; UAS-ex/ex<sup>697</sup>; dpp-Gal4, UAS-GFP/UAS-dia<sup>CA</sup>*, (C) *yw; UAS-hpo/ex<sup>697</sup>; dpp-Gal4, UAS-GFP/+*, (D) *yw; UAS-hpo/ex<sup>697</sup>; dpp-Gal4, UAS-GFP/UAS-dia<sup>CA</sup>*, (E) *yw; UAS-wts/ex<sup>697</sup>; dpp-Gal4, UAS-GFP/+*, (F) *yw; UAS-wts/ex<sup>697</sup>; dpp-Gal4, UAS-GFP/UAS-dia<sup>CA</sup>*.

Figure S2:

(A) *yw; ex<sup>697</sup>/+*; (B) *w; ap-Gal4, ex<sup>697</sup>/+; cpb<sup>RNAi</sup>/+*, (C) *yw; ex<sup>697</sup>/+; hh-Gal4, UAS-GFP/UAS-cpb<sup>RNAi</sup>*.

Figure S3:

(A) *yw; ex<sup>697</sup>/+; hh-Gal4, UAS-GFP/+*, (B) *yw; UAS-cpa<sup>RNAi</sup>/ex<sup>697</sup>; hh-Gal4, UAS-GFP/+*.

Figure S4:

(A) *yw; en-Gal4/+; diap1-GFP/+*, (B) *yw; en-Gal4/UAS-cpa<sup>RNAi</sup>; diap1-GFP/+*, (C) *yw; ex<sup>697</sup>/+; dpp-Gal4, UAS-GFP/+*, (D) *yw; ex<sup>697</sup>/UAS-cpa<sup>RNAi</sup>; dpp-Gal4, UAS-GFP/+*, (E-F) *yw; ex<sup>697</sup>/+; hh-Gal4, UAS-GFP/ UAS-wts<sup>RNAi</sup>*.

Figure S5:

(A) *yw, hs-flp; act<CD2<Gal4, UAS-GFP, ex<sup>697</sup>/UAS-cpa<sup>RNAi</sup>; UAS-bsk<sup>DN</sup>/+*, (B) *yw; ex<sup>697</sup>/+;hh-Gal4, UAS-GFP/UAS-bsk<sup>DN</sup>*, (C) *yw; UAS-cpa<sup>RNAi</sup>/ex<sup>697</sup>; hh-Gal4, UAS-GFP/UAS-bsk<sup>DN</sup>*.

Figure S6:

(A) *yw; UAS-cpa<sup>RNAi</sup>/ex<sup>697</sup>; hh-Gal4, UAS-GFP/UAS-w<sup>RNAi</sup>*, (B) *yw; UAS-cpa<sup>RNAi</sup>/ex<sup>697</sup>; hh-Gal4, UAS-GFP/UAS-GFP*, (C) *yw; ex<sup>697</sup>/+; hh-Gal4, UAS-GFP/UAS-yki<sup>RNAi</sup>*, (D) *yw; UAS-cpa<sup>RNAi</sup>/ex<sup>697</sup>; hh-Gal4, UAS-GFP/UAS-yki<sup>RNAi</sup>*, (E) *yw;ex<sup>697</sup>/+; dpp-Gal4, UAS-GFP/UAS-yki<sup>RNAi</sup>*, (F) *yw; ex<sup>697</sup>/+; dpp-Gal4, UAS-GFP/UAS, UAS-dia<sup>CA</sup>, UAS-yki<sup>RNAi</sup>*.

Figure S7:

(A-F) *yw; UAS-cpa<sup>RNAi</sup>/+; hh-Gal4, UAS-GFP/+*, (E) *w; ap-Gal4/+*; (F) *w; ap-Gal4/cpa<sup>RNAi</sup>*; (G) *w; ap-Gal4/+*; (H) *w; ap-Gal4/cpa<sup>RNAi</sup>*.

Figure S8:

(A-G) *yw; 30A-Gal4/+; UAS-dia<sup>CA</sup>/UAS-GFP*.

Figure S9:

(A-C) *yw; UAS-cpa<sup>RNAi</sup>/+; hh-Gal4, UAS-GFP/+*.

Figure S10:

(A) *w; nub-Gal4/+*; (B) *w; nub-Gal4/UAS-ex*; (C) *w; nub-Gal4/UAS-hpo<sup>ATG6</sup>*; (D) *w; nub-Gal4/UAS-wts*; (E) *yw; UAS-ex/ex<sup>697</sup>; dpp-Gal4, UAS-GFP/+*, (F) *yw; UAS-ex/ex<sup>697</sup>; dpp-Gal4, UAS-GFP/UAS-dia<sup>CA</sup>*, (G) *yw; UAS-hpo/ex<sup>697</sup>; dpp-Gal4, UAS-GFP/+*, (H) *yw; UAS-hpo/ex<sup>697</sup>; dpp-Gal4, UAS-GFP/UAS-dia<sup>CA</sup>*, (I) *yw; UAS-wts/ex<sup>697</sup>; dpp-Gal4, UAS-GFP/+*, (J) *yw; UAS-wts/ex<sup>697</sup>; dpp-Gal4, UAS-GFP/UAS-dia<sup>CA</sup>*.

Figure S11:

(A) *yw; UAS-ex/ex<sup>697</sup>; dpp-Gal4, UAS-GFP/UAS-dia<sup>CA</sup>*, (B) *yw; UAS-hpo/ex<sup>697</sup>; dpp-Gal4, UAS-GFP/UAS-dia<sup>CA</sup>*, (C) *yw; UAS-wts/ex<sup>697</sup>; dpp-Gal4, UAS-GFP/UAS-dia<sup>CA</sup>*.

Figure S12:

(A) *yw, hs-FLP; FRT40A cpb<sup>M143</sup>/FRT40A ubi-GFP*; (B) *yw, hs-FLP; FRT40A ex<sup>e1</sup>/FRT40A ubi-GFP*; (C) *yw, hs-FLP; FRT40A ft<sup>422</sup>/FRT40A ubi-GFP*.

### **Supplemental table and Figure legends**

#### **Table S1. Data of the Yorkie-Gal4 DNA binding domain, UAS-luciferase based screen.**

The data from the primary genome-wide Yki-GDBD + UAS-luc screen. For each condition, we indicate the plate, well, AmbionID of the dsRNA, the gene ID, the Firefly luciferase activity, the Renilla luciferase control activity and the ratio of the two. Each of the conditions is the average of a triplicate experiment. For the control conditions (knockdown of Diap1, ex/ft, Luc and Hpo) we use our own dsRNA constructs and no AmbionID is given. NA = not annotated.

#### **Figure S1. Validation and specificity controls for the Yorkie-luciferase activity assay in S2 cells**

(A) Luciferase activity assay of *Yki-Gal4 DNA binding domain (GDBD)* with or without cotransfection of *HA-Ex* and in the presence or absence of dsRNA as

indicated. Transfection of GDBD alone does not induce Luciferase activity (lane1). *lacZ RNAi* has no effect on Yki activity with or without cotransfection of *HA-Ex* (lanes 2-5). As control for the delivery of dsRNA into cells, Luciferase activity of Yki-GDBD transfected cells was measured in the presence of firefly Luciferase dsRNA (lane 6), which completely abolishes the signal. To validate the sensitivity of the assay to knockdown of known Hippo pathway components, Yki activity was measured in the presence of dsRNAs targeting *ex*, *hpo*, and *wts*. As shown (lanes 7-9), dsRNA against *ex*, *hpo* or *wts* rescued the suppression of the Yki activity by *HA-Ex*. **(B)** Luciferase activity assay of *sc-GDBD* cotransfected with *HA-Ex* and in the presence of dsRNAs as indicated. Knock-down by dsRNA targeting actin modulators or Hpo pathway components like *ex*, *hpo* and *wts* did not cause significant upregulation of *sc-GDBD* activity.

**Figure S2. Knockdown of Capping protein B *in vivo* causes overgrowth and activation of Hpo target genes**

Third instar wing discs. (A-C) *ex-lacZ* staining (red and gray) and GFP (green) of the indicated genotypes. Knockdown of Cpb caused up-regulation of *ex-lacZ* expression and overgrowth in the dorsal **(B)** and posterior **(C)** compartments where *ap-Gal4* and *hh-Gal4*, respectively, are expressed.

**Figure S3. Knockdown of Capping Protein A caused overgrowth of the hinge region**

Third instar wing discs. **(A,B)** Vestigial (Vg) staining (red and gray) and GFP (green) of the indicated genotypes. Vg staining was used to mark the pouch region. Down-regulation of Cpa caused overgrowth of the presumptive hinge region in the *hh-Gal4* expression domain.

**Figure S4. Knockdown of Capping Protein A or expression of Dia<sup>CA</sup> causes overgrowth and activation of Hippo target genes in different tissues and mimics Warts knockdown phenotypes**

Third instar wing discs. **(A,B)** Ci staining (green) and Diap1-GFP (red and gray) of the indicated genotypes. Ci staining was used to label the anterior compartment and differentiate it from the posterior compartment where *en-Gal4* is expressed. **(B)** Knockdown of Cpa caused up-regulation of Diap1-GFP expression. **(C,D)** Third instar leg disc. *ex-lacZ* staining (red and gray) and GFP (green) of the indicated genotypes. **(D)** Dia<sup>CA</sup> expression caused up-regulation of *ex-lacZ* expression and overgrowth of the discs. **(E,F)** Third instar wing discs overexpressing *wts<sup>RNAi</sup>* in the posterior compartment driven by *hh-Gal4* stained for **(E)** *ex-lacZ* and **(F)** Wg staining (red and gray) and expression GFP (green) to mark the Gal4 expression domain. These results show that knockdown of Cpa or overexpression of Dia<sup>CA</sup> mimics the overgrowth and up-regulation of *ex-lacZ* in *wts* loss of function.

**Figure S5. Expression of *bsk<sup>DN</sup>* does not affect *ex-lacZ* expression**

Third instar wing discs. **(A)** *Flip-out-Gal4* clones expressing *UAS-bsk<sup>DN</sup>*. GFP marks the overexpression clones (GFP: green), *ex-lacZ* (red and gray). *ex-lacZ* is not affected by expression of *bsk<sup>DN</sup>*. **(B)** Similarly, overexpression of *UAS-bsk<sup>DN</sup>* using *hh-Gal4*, which is marked by GFP overexpression (green), does not affect *ex-LacZ* expression (red and gray). **(C)** Experiment to test whether JNK signaling is required for the upregulation of *ex-lacZ* expression upon knockdown of Cpa. *ex-lacZ* staining (red and gray) and GFP marking the *hh-Gal4* overexpression domain (green) indicating that JNK is not required for the upregulation of *ex-lacZ*.

**Figure S6. Yorkie is required for actin dynamics induced overgrowth and upregulation of Hippo target genes**

Third instar wing discs of the indicated genotypes. **(A-B)** The addition of a benign dsRNA targeting the *white* gene or an extra copy of *UAS-GFP* has no effect on the *cpa<sup>RNAi</sup>* induced *ex-lacZ* (red and gray) upregulation and overgrowth. **(C-F)** Wg staining (red and gray) and GFP (green) of the indicated genotypes. **(C)** Wg expression is not affected by knockdown of Yki. **(D)** The up-regulation of Wg caused by the knockdown of Cpa (Fig. 3F) is suppressed by concomitant knockdown of Yki. **(E)** Wg expression is not affected by *dpp-Gal4* driven knockdown of Yki. **(F)** The up-regulation of Wg caused by expression of *Dia<sup>CA</sup>* (Fig. 3H) is suppressed by the concomitant knockdown of Yki.

**Figure S7. Knockdown of Cpa does not markedly affect cell polarity and Hh and Dpp signaling**

Third instar wing discs. **(A-F)** Confocal cross sections analyzing antibody stainings for apical-basal polarity markers in *hh-Gal4*, *UAS-cpa<sup>RNAi</sup>*, *UAS-GFP* (green) discs. **(A)** Armadillo, **(B)** E-Cadherin, **(C)** Patj, **(D)** Crumbs, **(E)** Dlg and **(F)** Phalloidin (red and gray) staining. While F-actin levels are increased, cell polarity does not seem to be significantly affected by knockdown of Cpa. **(F)** Phalloidin staining (red and gray) and GFP (green). F-actin is induced by knockdown of Cpa. **(G,H)** Staining for phosphorylated Mad (p-Mad) in **(G)** *ap-Gal4* and **(H)** *ap-Gal4*, *UAS-cpa<sup>RNAi</sup>* wing discs. p-Mad expression is not significantly affected by the knockdown of Cpa. **(I,J)** Cubitus interruptus (Ci) staining **(I)** *ap-Gal4* and **(J)** *ap-Gal4*, *UAS-cpa<sup>RNAi</sup>* wing discs. Ci expression did not significantly change upon the knockdown of Cpa. These results show that loss of Capping proteins does not cause a general defect in cell signaling and cell polarity.

**Figure S8. Overexpression of Dia<sup>CA</sup> causes severe overgrowth and folding of the epithelium but has limited effects on epithelial cell polarity and Hh and Dpp signaling**

Third instar wing discs overexpressing Dia<sup>CA</sup> in the presumptive hinge region by *30A-Gal4*. **(A-E)** Optical cross-sections stained for apical-basal polarity markers. GFP (green) and Dapi (blue). **(A)** E-Cadherin, **(B)** Patj, **(C)** Crumbs and **(D)** Dlg (red and gray, E'). The localization of these markers was not significantly affected in the cells that stayed in the epithelium, although some mutant cells left the epithelium and had abnormal Dapi staining. **(E)** Staining for phosphorylated Mad



(red and gray). p-Mad expression pattern is still apparent upon  $\text{Dia}^{\text{CA}}$  overexpression. **(F)** Cubitus interruptus (Ci) staining (red and gray). Ci expression is still higher along the compartment border upon  $\text{Dia}^{\text{CA}}$  overexpression. These results show that although  $\text{Dia}^{\text{CA}}$  overexpression causes dramatic folding and the extrusion of some cells out of the epithelium, epithelial polarity markers are still correctly localized and there is no general defect in cell signaling.

**Figure S9. The induction of F-actin polymerization does not notably affect the localization of Hippo pathway components.**

Optical cross-sections of third instar wing discs with knockdown Cpa by *hh-Gal4*, which is marked by GFP expression (green). **(A)** Mer (red and gray), **(B)** Ex (red and gray) and **(C)** Hpo (red and gray) localization was not significantly affected upon knock-down of Cpa.

**Figure S10. Overgrowth and up-regulation of Hippo target genes by  $\text{Dia}^{\text{CA}}$  is suppressed by co-overexpression of Warts**

**(A-D)** adult wings. The wing specific driver *Nubbin-Gal4* **(A)** was used to overexpress Ex, Hpo and Wts **(B-D)**. Overexpression of Ex or Hpo caused stronger growth reduction than overexpression of Wts. **(E-J)** Wg staining (red and gray) and GFP (green) of wing discs of the indicated genotypes. The Wg expression pattern was not affected by overexpression of **(E)** Ex, **(G)** Hpo or **(I)** Wts. Co-expression of **(F)** Ex or **(H)** Hpo with  $\text{Dia}^{\text{CA}}$  did not suppress  $\text{Dia}^{\text{CA}}$ -caused induction of ectopic Wg expression and tissue overgrowth. In contrast,

overexpression of **(J)** Wts suppressed the Dia<sup>CA</sup>-induced upregulation of Wg and tissue overgrowth.

**Figure S11. Overexpression of Expanded, Hippo or Warts does not inhibit the induction of F-actin polymerization caused by Dia<sup>CA</sup> expression**

Third instar wing discs of indicated genotypes. GFP (green, gray in A'-C') and Phalloidin (red, gray in A''-C''). Dia<sup>CA</sup> coexpressed with **(A)** Ex, **(B)** Hpo and **(C)** Wts. The overexpression of Ex, Hpo or Wts does not affect the induction of F-actin formation by Dia<sup>CA</sup>.

**Figure S12. F-actin levels in *cpb*, *ex* and *fat* mutant clones**

Optical cross-sections of third instar wing discs containing mutant clones marked by the absence of GFP expression (green), F-actin is marked by Phalloidin staining (red and gray). **(A)** *cpb*<sup>M143</sup> mutant cells showed a marked increase in F-actin levels. **(B)** *ex*<sup>e1</sup> mutant clones showed some increase in F-actin levels, but not as severe as *cpb* mutant cells. **(C)** *ft*<sup>422</sup> mutant clones showed no significant alteration in F-actin levels.

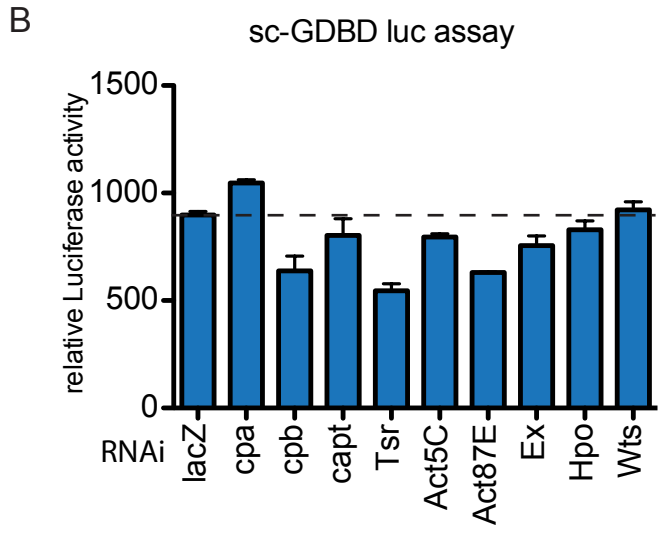
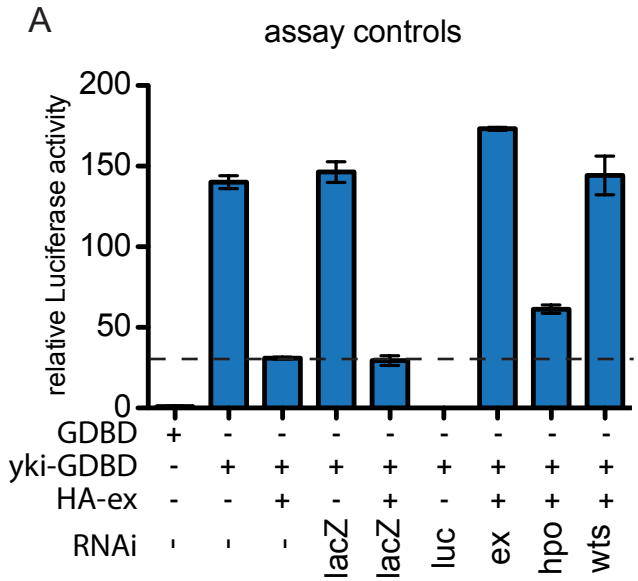


Figure S1

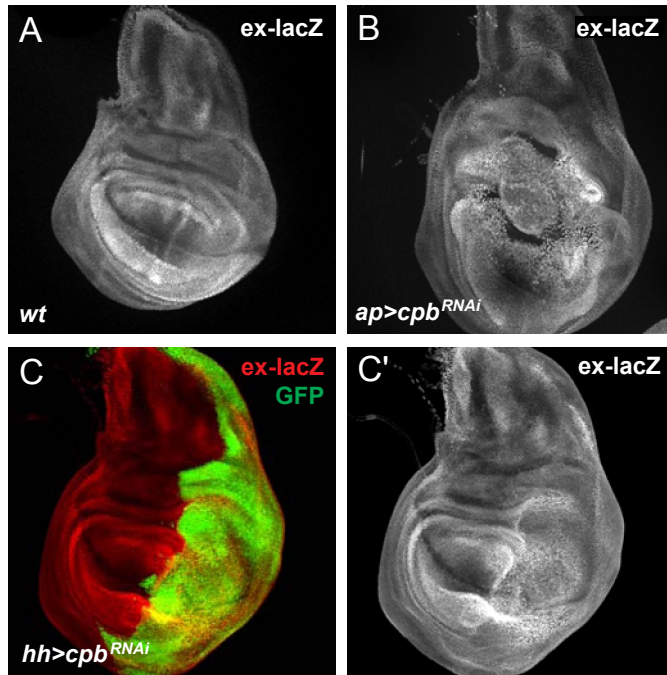


Figure S2

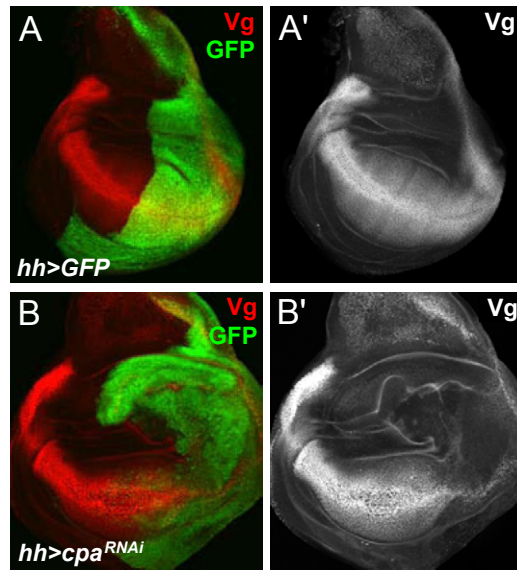


Figure S3

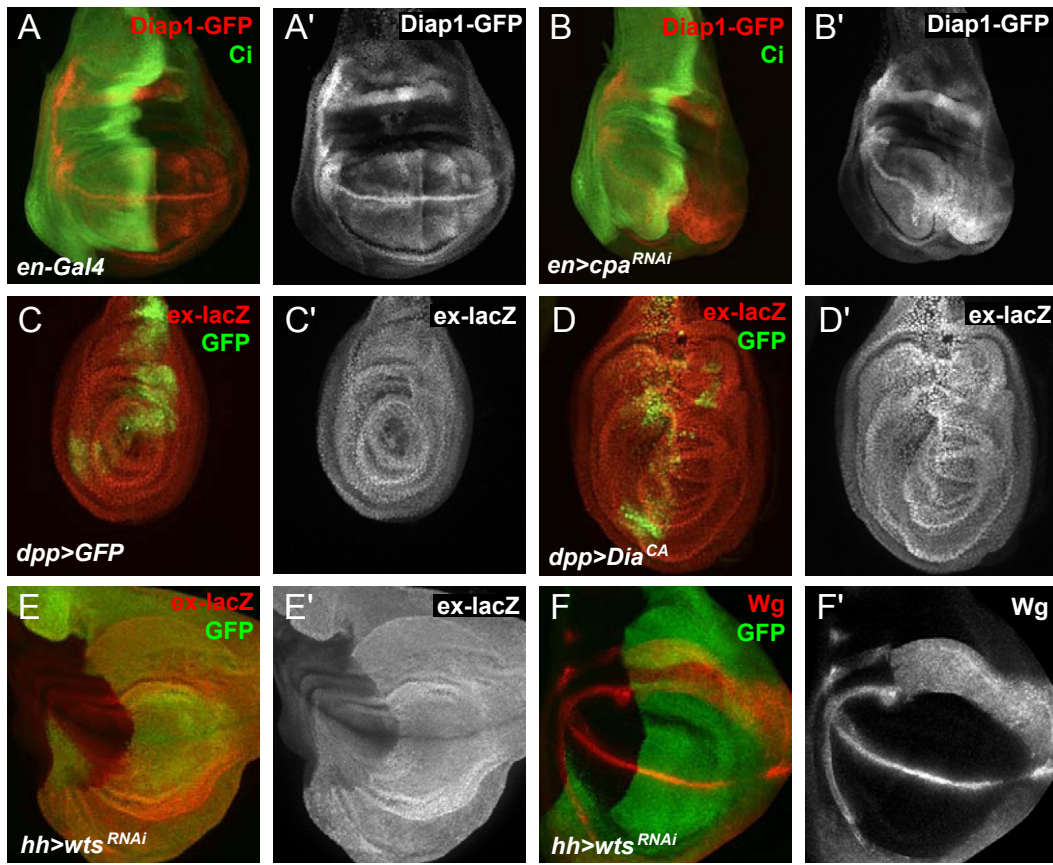


Figure S4

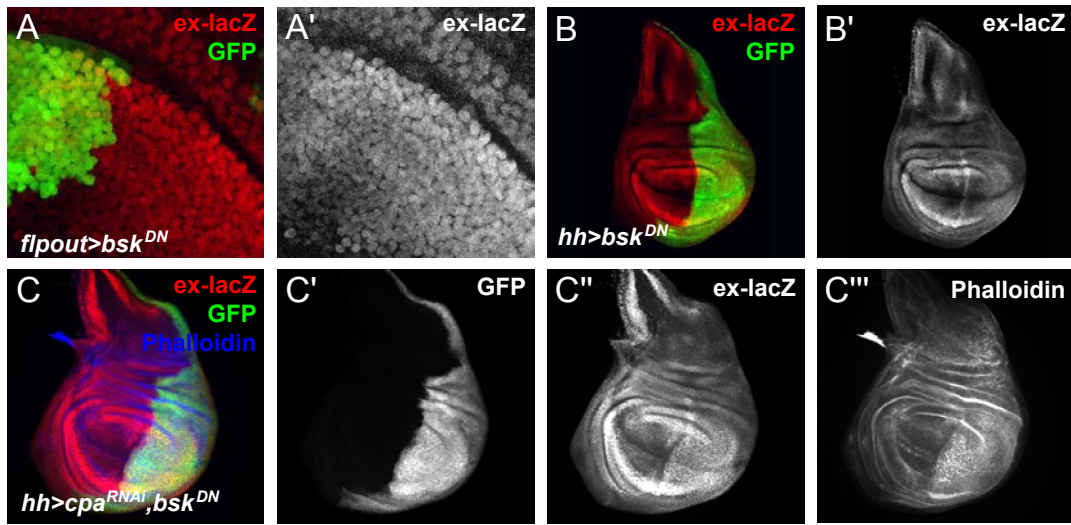


Figure S5

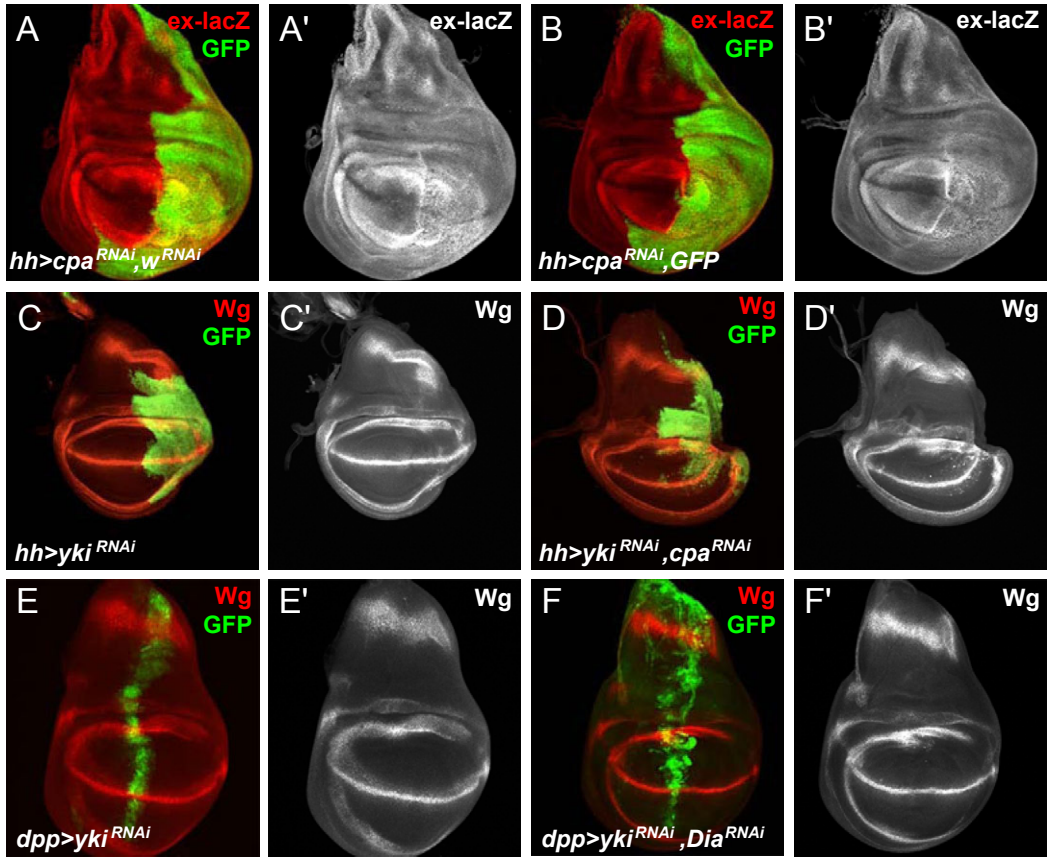


Figure S6



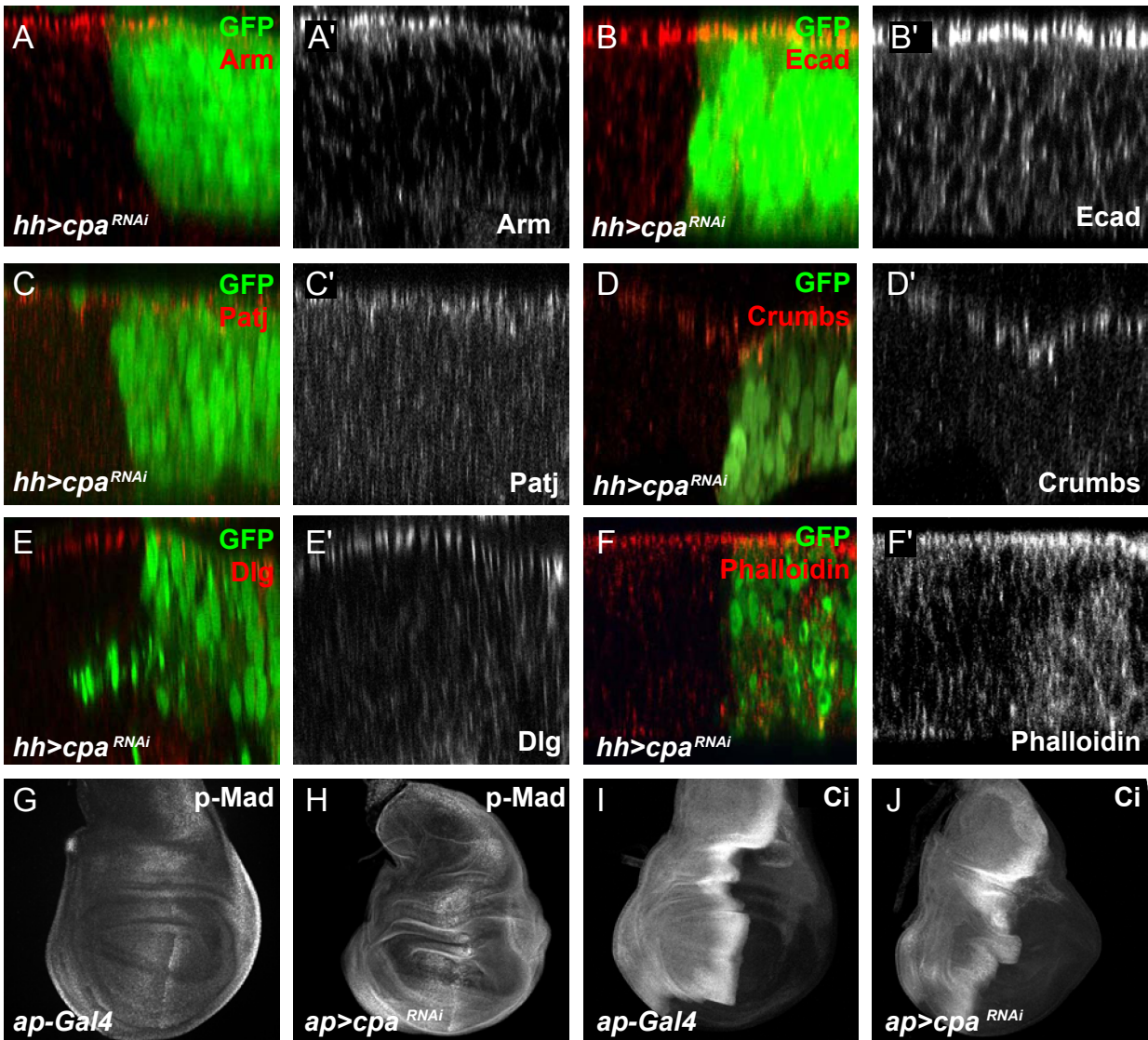


Figure S7

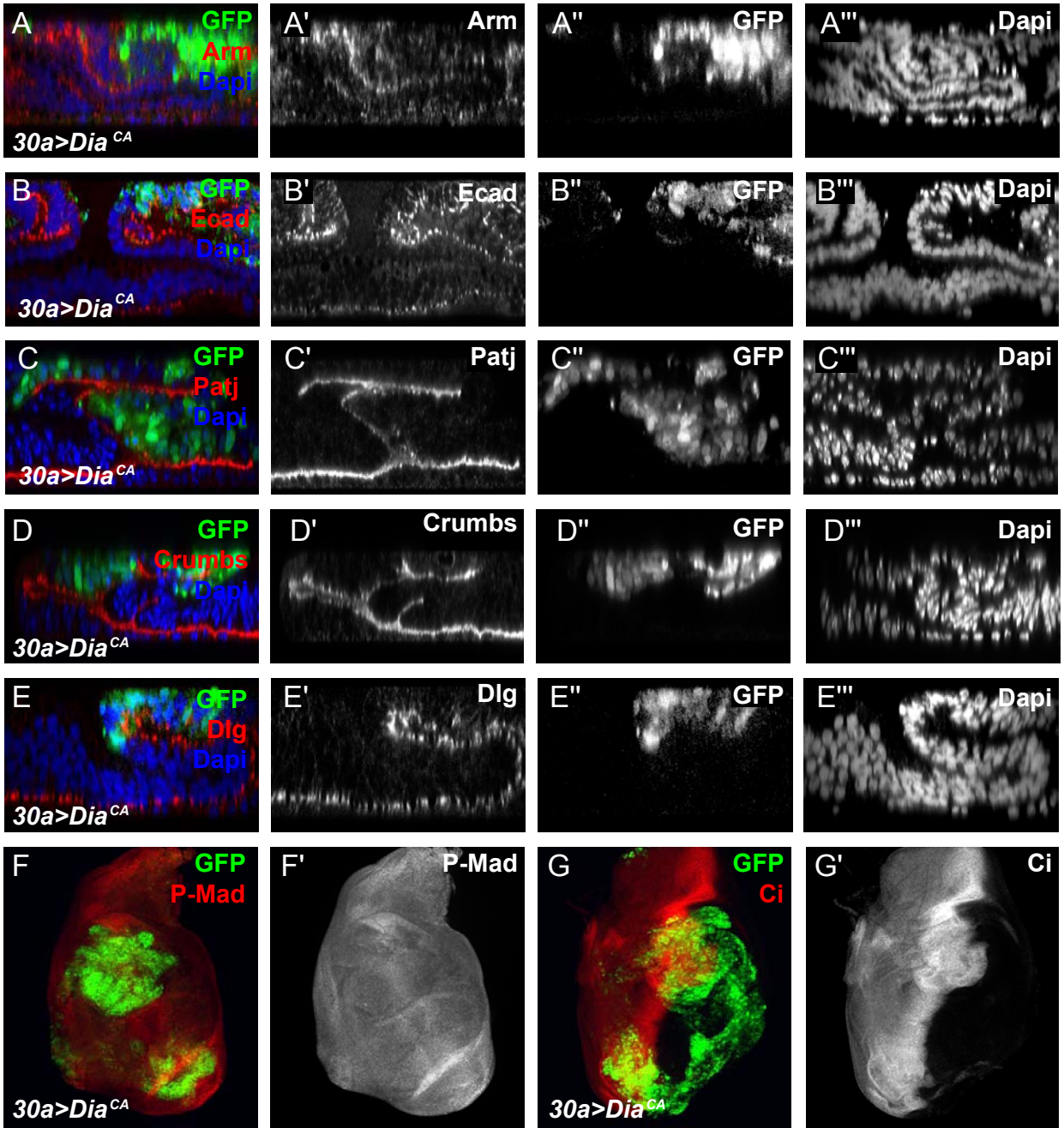


Figure S8

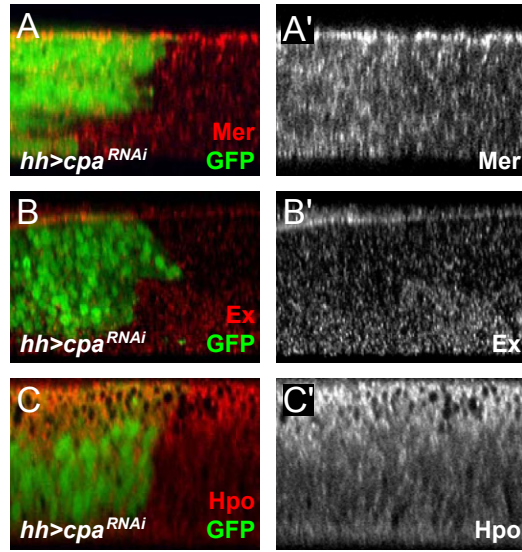


Figure S9

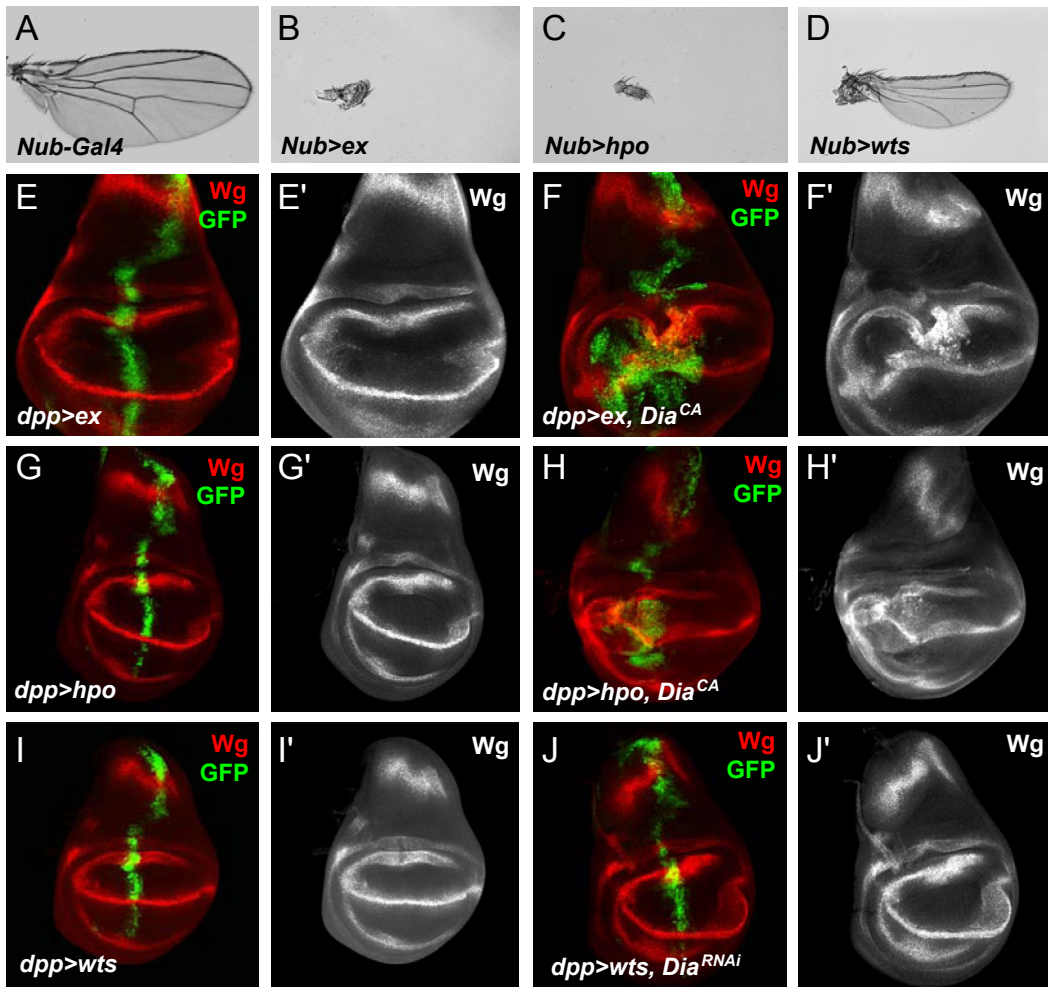


Figure S10



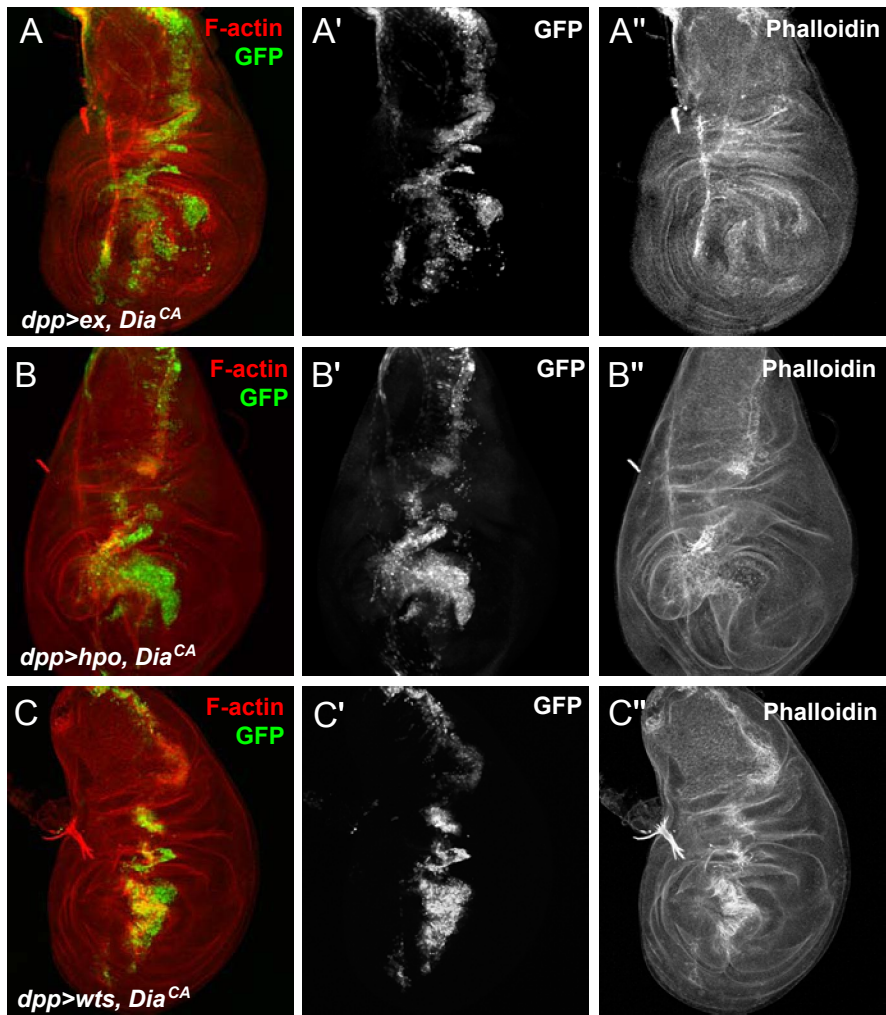


Figure S11

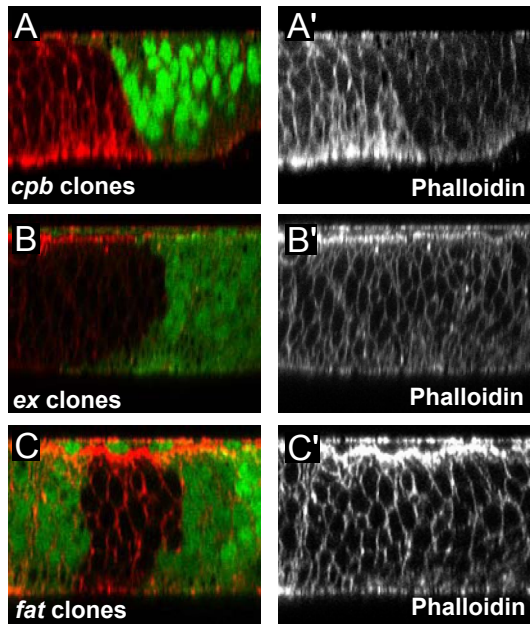


Figure S12